

# Applying the HPT-GWS for Hydrostratigraphy, Water Quality and Aquifer Recharge Investigations

by Wesley McCall, Thomas M. Christy, and Mateus K. Evald

---

## Abstract

The primary objective of this study was to evaluate use of the hydraulic profiling tool-groundwater sampler (HPT-GWS) log data as an indicator of water quality (level of dissolved ionic species) in an alluvial aquifer. The HPT-GWS probe is designed for direct push advancement into unconsolidated formations. The system provides both injection pressure logs and electrical conductivity (EC) logs, and groundwater may be sampled at multiple depths as the probe is advanced (profiling). The combination of these three capabilities in one probe has not previously been available. During field work it was observed that when HPT corrected pressure ( $P_c$ ) indicates a consistent aquifer unit then bulk formation EC can be used as an indicator of water quality. A high correlation coefficient ( $R^2 = 0.93$ ) was observed between groundwater specific conductance and bulk formation EC in the sands and gravels of the alluvial aquifer studied. These results indicate that groundwater specific conductance is exerting a controlling influence on the bulk formation EC of the coarse-grained unit at this site, and probably many similar sites, consistent with Archie's Law. This simple relationship enables the use of the EC and  $P_c$  logs, with targeted water samples and a minimum of core samples, to rapidly assess groundwater quality over extended areas at high vertical resolution. This method was used to identify both a brine impacted zone at the base of the aquifer investigated and a groundwater recharge lens developing below storm water holding ponds in the upper portion of the same aquifer. Sample results for trace level, naturally occurring elements (As, Ba, U) further demonstrate the use of this system to sample for low level groundwater contamination.

---

## Introduction and Background

Direct push (DP) injection logging has been under development for investigation of unconsolidated formations for several years (Pitkin et al. 1999; Chapuis and Chenaf 2003; Butler et al. 2007; Dietrich et al. 2008; Kober et al. 2009; McCall et al. 2009, 2014; Reiffsteck et al. 2010; Geoprobe 2011a; Liu et al. 2011; Dietze and Dietrich 2012). The hydraulic profiling tool (HPT) is an injection probe that has one screened port on the side of the probe. Clean water is injected through the port into the formation as the probe is advanced (Geoprobe 2013; ASTM 2016). A transducer located down hole, just above the probe, is used to monitor the pressure required to inject water into the formation. Clean, coarse grained unconsolidated materials such as sands and gravels usually require very little pressure (<2 to 5 psi above hydrostatic pressure) to inject the water. Finer

grained materials such as silts and clays may result in injection pressures ranging from 20 psi to 100+psi. (It should be noted that injection at high pressures in fine-grained or cemented materials at shallow depths may result in fracturing of the formation when lithostatic pressure is exceeded or can cause bypass of water along the drive rods. This occurs primarily when probe advancement is halted.) Of course, mixtures of fine to coarse grained materials occur in nature resulting in varying injection pressures depending on the grain size distribution of the mixture and degree of compaction, etc. HPT pressure logs are used to assess variations in formation permeability and sediment type. HPT logging is often used during contaminant investigations to define and track potential contaminant migration pathways (Pitkin et al. 1999; McCall et al. 2014) or for hydrogeologic and water resources investigations (McCall et al. 2009; Geoprobe 2011a). Cross sections of HPT logs may be used for developing models of geology/hydrostratigraphy and to support development of high resolution site models (Kober et al. 2009; McCall et al. 2009, 2014).

At least one multi-port injection logging tool (Pitkin et al. 1999) has been used since 1995 for both injection logging and sampling groundwater as the probe is advanced. The single port HPT probe and similar tools did not allow for

---

*Article impact statement:* A new DP logging-groundwater profiling tool is used to define water quality, brine impact, and aquifer recharge in an unconsolidated aquifer.

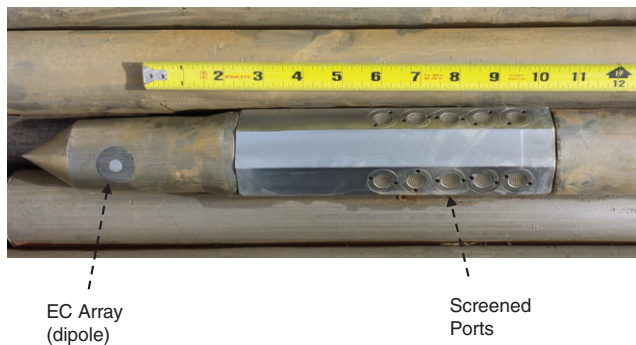


**Figure 1. The HPT-GWS probe is designed with 20 screened ports that are approximately 0.4-inches (10 mm) in diameter. This probe is constructed with a simple electrical conductivity dipole array for measuring bulk formation electrical conductivity. It is designed to be driven with 2.25" (57 mm) diameter probe rods. Ruler scale is in inches.**

sampling during the logging operation. However, the HPT-GWS probe (Figure 1) has been designed with multiple ports to permit sampling at targeted depths in permeable zones of an unconsolidated formation as the probe is advanced. To facilitate sampling a separate and replaceable sample line is attached to the probe. Also, the increased number of screened ports (20) provides for more screened surface area and better groundwater yield from permeable formations.

Resistivity arrays or their inverse, electrical conductivity (EC) arrays, have been used to measure bulk resistivity or electrical conductance of consolidated and unconsolidated formations and soils (Dobrin 1976; Rhoades and Schilf-garde 1976; Keys 1997; Hallenberg 1998). Several factors influence the electrical conductivity of soils and unconsolidated materials. Some of these include mineralogy, clay content, degree of saturation, level of dissolved ions in the contained water, etc (Milsom and Eriksen 2015).

In DP logging the EC array is advanced directly into the unconsolidated formation, without a pre-existing borehole or well or the use of drilling fluids. The electrodes of the array are in intimate contact with the formation so that no correction for borehole or well diameter, drilling fluid conductance, or mud invasion is required. In fresh water formations the DP EC log, along with other information (e.g.,  $P_c$  logs and/or targeted core samples) often is used to help define sediment type and hydrostratigraphy (Christy et al. 1994; Schulmeister et al. 2003; McCall et al. 2009, 2014). In unconsolidated formations dry, coarse materials such as siliceous sand and gravel, usually exhibit very low electrical conductivity (e.g.,  $<3$  mS/m). Clean silts and fine sandy silts also may exhibit low electrical conductance. Clays typically exhibit a relatively high EC (100 to 300+ mS/m) and in fresh water settings clay content often controls the bulk formation EC of unconsolidated formations (Christy et al. 1994; Schulmeister et al. 2003). However, some clay minerals do not exhibit high electrical conductance and this can complicate lithologic interpretation based solely on EC when these types of clays are present in the area being investigated (McCall et al. 2014). When high levels of ionic contaminants such as salt (NaCl) are dissolved in groundwater they can cause elevated bulk EC readings (e.g.,  $>500$  mS/m) even

in sands and gravels. The presence of even modest levels of ionic contaminants in groundwater can overwhelm and mask natural formation EC responses making it difficult if not impossible to interpret formation type based solely on EC. Under these conditions running an HPT log in tandem with an EC log can provide insight into formation type, as well as permeability, as HPT injection pressure is essentially insensitive to the ionic content of groundwater. Owing to its sensitivity to ionic contaminants, an EC array can be useful for locating and tracking ionic contaminants (brine, sea water, etc.) or some remediation injectates (e.g., persulfate) under many conditions. In fact, we will demonstrate here that bulk formation EC contrasted to corrected HPT pressure ( $P_c$ ) can be used to identify and map changes in water quality due to the dissolved ion content in clean, saturated sands and gravels that make up many unconsolidated aquifers.

The area where the logging and sampling for this project was conducted is located on an alluvial flood plain near the confluence of the Smoky Hill and Saline Rivers in Saline County, Kansas (Figure 2). The Quaternary Age alluvial deposits at this location consist of an upper fine grained unit ranging from a few inches to over 40 ft in thickness in some areas. The permeability of the fine-grained unit may be  $<1 \times 10^{-6}$  cm/s in clay rich zones (KGS 1949). The fine-grained unit usually contains varying amounts of silt and sand mixed with clay and the permeability increases with increasing silt/sand content. Below the fine-grained unit is a coarse-grained unit that ranges from a few feet to over 80 ft in thickness across the river basin. The coarse-grained unit consists largely of siliceous sand and gravel with minor amounts of intermixed silt and clay. Permeability in the coarse-grained "aquifer" unit may exceed  $1 \times 10^{-2}$  cm/s in some zones (KGS 1949). Discontinuous silt-clay layers from  $<1$ -inch (2 cm) thick to over 5 ft (1.5 m) in thickness are randomly distributed within the coarse-grained unit. The Quaternary alluvium unconformably overlies the Permian Age, Ninnescah Shale in this area. The shale may exceed 500 ft in thickness and thin beds of limestone and silt-sandstone do occur. Blebs, crystals and layers of gypsum are not uncommon in the shale and the Permian Age formation is mined for salt some miles south and west of the field area (KGS 1949). West of the study area the Saline River flows across and cuts through the Cretaceous Age Dakota formation. The connate water in some zones of the Dakota formation contain high levels of salts which may have contributed to the salty nature and thus the name of the Saline River (KGS 1952).

## Equipment and Methods

An HPT-GWS probe (Model KS8050; Geoprobe, Salina, Kansas) was used to perform logging and groundwater profiling for this investigation (Geoprobe 2013). The probe was equipped with 20 screened ports in 4 groups of 5 screens spaced at  $90^\circ$  intervals over an approximately 4-inch (100 mm) long section of the probe (Figure 1). The screened area for each port is about 0.4-inches (10 mm) in diameter and the screens can be replaced if damaged. Logging was performed with a DP machine by advancing the probe at approximately 2 cm/s ( $\sim 4$  ft/min) while water was injected at approximately 400 mL/min through the ports. The pressure required to

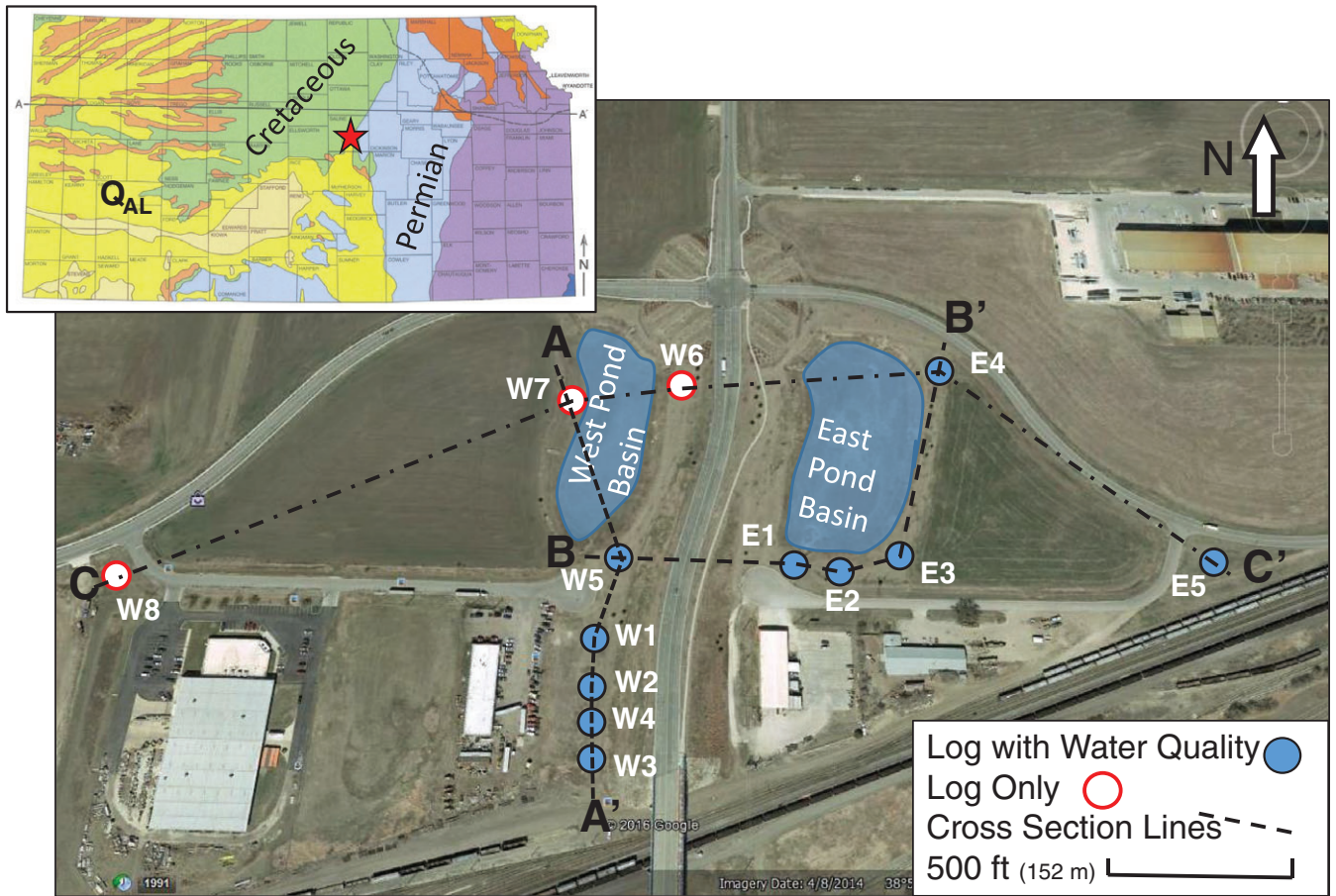


**Figure 2.** Site map with log-sample locations and site features. Red star gives approximate site location on inset geologic map.  $Q_{AL}$  = Quaternary Age alluvial deposits. Aerial photo from Google Earth Maps. Generalized Geologic Map of Kansas after the Kansas Geological Survey (2000).

inject water into the formation was measured by an in-line pressure sensor (Model 210091; Geoprobe) placed just a few inches above the probe in the connection rod. A polymer clad trunkline containing all electrical wires for the down-hole sensors and the injection flow tube was pre-strung through the drive rods before logging was started. The trunkline connected the down-hole sensors to the up-hole electronics package and injection pump. The electronics package included a Field Instrument (Model FI6000; Geoprobe), HPT Flow Module (Model K6300; Geoprobe), and a laptop computer with acquisition software. Injection flow rate was controlled by the HPT Flow Module and flow rate and line pressure were measured and logged with depth. The Field Instrument (FI) received analog input from the down-hole pressure and EC sensors and the HPT Flow Module and converted the signal to digital output communicated to the laptop computer. Pressures, flow rate, EC, depth and rate of penetration were displayed on screen using the acquisition software. The data were logged with depth and saved to file for later review, presentation and reporting. Before and after each log a quality assurance test (Geoprobe 2013; ASTM 2016) was conducted to verify that the pressure sensor, EC array, and instrumentation were operating correctly and providing accurate data. QA test results were saved with the log data files.

Depth of the probe below ground surface was tracked with a string potentiometer mounted on the DP machine.

The DP machine weight, hydraulic slides, and percussion hammer were used to drive the probe into virgin, unconsolidated materials. The EC array and injection screens were in intimate contact with the formation as the probe was advanced. Fluid pressure behind the screens prevents clogging and injection pressure and bulk formation EC were logged every 0.05 ft (~15 mm) as the probe was advanced. Once the operator reached the desired depth, or refusal was encountered, the machine hydraulics were used to retract the probe while maintaining fluid flow to keep the injection screens open.

The HPT pressure and EC logs were observed as the probe was advanced into the formation to guide selection of groundwater sampling intervals. Once the probe was in saturated materials groundwater sampling could be performed. The presence of low HPT injection pressure was the primary guide to high permeability zones where the formation would yield sufficient water for sampling. At this site, low permeability materials exhibited both high HPT pressure and high EC and would not yield sufficient water for sampling. (As noted above not all clay minerals exhibit high EC, so in some areas EC can be low when HPT pressure is high, indicating low permeability.) Additionally, when  $P_c$  was low and flat, changes in bulk formation EC provided indications of changes in water quality, and was used to further refine selection of groundwater sample intervals.



A small diameter mechanical bladder pump (McCall 2005; Geoprobe 2011b) was used to perform purging and groundwater sampling with this system. Before advancement the pump was attached to the sample line from the HPT probe and suspended a few feet above the probe in the drive casing. Once at the desired sampling depth(s) probe advancement was halted and the HPT injection flow was stopped. A “time file” was started in the acquisition software to monitor pressure vs. time, and a pressure dissipation test was performed (Figure S1, Supporting Information). A 12V electrical actuator was then mounted on the top of the drive rods and the sample line was attached to the actuator. The actuator raises and lowers the sample line which opens and closes the corrugated bladder in the pump, pumping water to the surface. Flow rates varied from about 300 mL/min to <100 mL/min depending on depth and formation permeability. A peristaltic pump may be used for sampling when depth to groundwater is shallow (<25 ft).

Sample flow was directed to the flow cell of a water quality meter (Model 556 MPS; YSI Inc., Yellow Springs, Ohio) where specific conductance, pH, dissolved oxygen (DO), and oxidation-reduction potential (ORP) were monitored to stability (Figure S2). Time for parameter stabilization ranged from about 15 min to over 30 min depending primarily on the flow rate obtained. Turbidity measurements were periodically taken during the purging process (Oakton Model T100; Cole-Parmer, Vernon Hills, Illinois). All samples for cation, anion, and trace element (arsenic, barium, uranium) analysis were filtered with a 0.45  $\mu$  filter (Model EW-99157-50; Cole-Parmer) and collected in properly preserved sample bottles. Analyses were performed by Pace Analytical Laboratory (Salina, Kansas) using approved state and EPA methods for the selected analytes.

## Results and Discussion

### Water Quality and Analytical Results

Below the water table, low HPT pressure was the primary guide used for the selection of permeable intervals for sampling. Variations of EC in low HPT pressure zones were used to assess changes in water quality to target desired intervals. With bulk formation EC increasing above background levels (~25 mS/m) indicating increases in brine impact and bulk formation EC falling below background levels indicating freshwater recharge. At the selected depths probe advancement was halted and HPT injection flow was turned off to conduct a dissipation test (Figure S1). Rapid pressure dissipation indicated that formation yield should be sufficient for sampling. Flow from the down-hole pump was directed through the flow cell of the water quality meter to monitor parameters to stability (Table S1 and Figure S2). A plot of specific conductance vs. depth for all groundwater samples at the site (Figure S3) reveals that brine impact to the groundwater occurred primarily below a depth of 75 ft (~23 m).

After the initial round of logging and water quality profiling two locations were selected to conduct sampling for major element cations and selected anions and trace elements (Table S2). The HPT-GWS probe was used to conduct this sampling as a second log was obtained at both locations.

The background location (E5) was sampled at three depth intervals (40, 60, and 84 ft) across the saturated aquifer to assess concentration trends vs. depth. The second location (E4) was sampled at six depth intervals guided by variations in the EC log and groundwater specific conductance data. A plot of the major element cations and anions vs. depth (Figure S4) reveals that concentration trends at the background location are relatively low and flat, with only minor variations in concentration. Conversely, at location E4 both cation and anion concentrations increase significantly with depth and mimic changes observed in the groundwater specific conductance (Table S1 and Figure S3).

Samples for uranium and arsenic were collected because these naturally occurring elements may be mobilized by changing redox and/or pH conditions (Smith et al. 2000; Welch et al. 2000; Sherman et al. 2007; McCall et al. 2009) which may occur during aquifer recharge. Modest increases in dissolved concentrations of these elements with maximum contaminant levels in the microgram per liter range (EPA 2001a, 2001b) can significantly impair the water quality of an aquifer storage and recovery (ASR) system. Here we see the concentration trends of uranium and barium vs. depth are similar at the background location and E4 location (Table S2 and Figure S5). Barium concentrations average almost a factor of 10 greater than uranium. Both elements exhibit slightly higher concentrations near the middle of the aquifer and decrease in the shallow and deeper zones of the formation. The highest concentrations of both elements occur at the background location. The highest uranium concentration was 22.8  $\mu$ g/L, below the 30  $\mu$ g/L maximum contaminant level (U.S. EPA, 2016). Arsenic was nondetect at the 5  $\mu$ g/L reporting level for all samples. Results of the trace element samples demonstrate that the HPT-GWS system also can be used to perform groundwater profiling for low level contaminant distribution investigations.

### Basic HPT Log Interpretation and Sediment Type

The initial log obtained at the site was at the W1 location (Figure 3). The HPT pressure in the top 25+ ft zone was relatively high, showing significant variation and reaching 50+ psi over two intervals. The EC log displays a similar trend across the upper 25+ ft mimicking the HPT pressure. Sampling nearby (ASTM 2015a) confirmed this was a silty to sandy clay-rich material. Just above 30 ft the HPT pressure drops to about 15 psi and then slowly increases with depth. The steady pressure increase with depth is piezometric pressure rise as the probe is advanced below the water table. Several pressure dissipation tests were run at different depths as the log was obtained. When stabilized the dissipation tests define the piezometric pressure at the given depth (Figure S1). Several stabilized dissipation pressures are plotted as triangles on the pressure log and define the piezometric pressure profile (Figure 3). Below 30 ft the piezometric profile is very close to the total HPT pressure measured over much of the log. This indicates that the formation is very permeable over most of this depth interval and coring nearby (ASTM 2015a) recovered sands with fine to coarse gravel. There are three distinct pressure peaks, one around 40 ft and two between 65 and 70 ft. These pressure peaks indicate the presence of clay layers in the otherwise

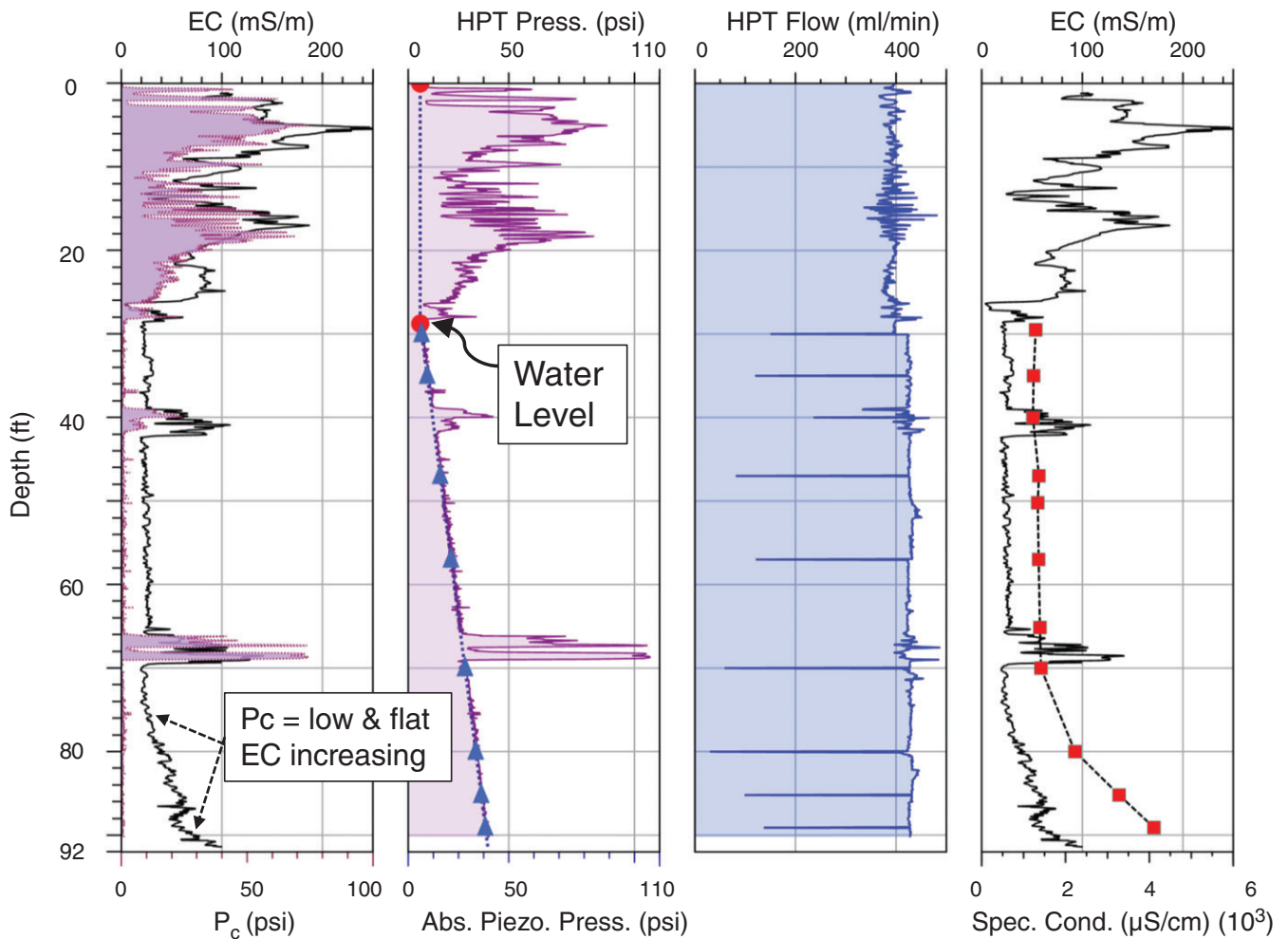


**Figure 3.** HPT-GWS log from location W1. Left to right: First panel is corrected HPT pressure ( $P_c$ /purple fill) plotted over bulk formation EC (black line/white fill). Second panel is total HPT pressure (pale purple fill) and piezometric profile (dotted line) with triangles plotted at each depth where a pressure dissipation test and/or sample was collected. Triangles mark the piezometric pressure at each depth. Third panel is HPT injection flow rate. Fourth panel is groundwater specific conductance (dashed line/red box) over bulk formation EC.

coarse-grained “aquifer” unit. Looking again at the EC log below 30ft we see that bulk formation EC is relatively flat over much of this interval with increased EC at the same depths where HPT pressure peaks occur. This independently confirms there are 3 clay layers at the given depths in the sand and gravel of the aquifer unit. There is minimal change in the HPT flow rate graph down the log. Flow rate will decrease in very low permeability formations. Downward spikes in the flow rate graph occurred where each pressure dissipation test was conducted and is an artifact of performing the dissipation tests.

During the QA test prior to running each log the atmospheric pressure was determined with the HPT pressure sensor. Given this and at least one stabilized dissipation test the water level can be calculated (Figure 3). Furthermore, the total HPT pressure ( $P_T$ ) can be corrected by subtracting the atmospheric ( $P_{atm}$ ) and piezometric ( $P_{piezo}$ ) pressure from the total HPT pressure measured at each depth increment (i) of the log. So, the corrected HPT pressure ( $P_c$ ) at each depth increment is:

$$P_{c(i)} = P_{T(i)} - (P_{piezo(i)} + P_{atm(i)})$$

The corrected HPT pressure is a function of the formation permeability. The  $P_c$  removes the atmospheric pressure and piezometric pressure rise from the HPT pressure log providing a clear representation of the changes in formation permeability vs. depth. Plotting the  $P_c$  log over the bulk formation EC log (Figure 3, left panel) allows us to see that the EC log and the corrected pressure log for this location mimic one another closely over most of the log profile, high in the clay-rich unit and clay lenses and low in the aquifer unit. However, below approximately 75 ft,  $P_c$  remains low and flat while the bulk formation EC increases. The flat  $P_c$  log over this interval verifies that the increase in bulk formation EC here is not due to an increase in clay content in the formation, which would lower permeability and result in increasing pressure. This condition of low, flat  $P_c$  with rising EC generally defines a positive EC anomaly (There can be exceptions: e.g., a fine sand and a silty-clayey medium sand may have similar permeabilities but different EC). When

the groundwater specific conductance measured at each depth in the formation is plotted over the bulk formation EC (Figure 3, right panel) it is evident that as the groundwater specific conductance increases, the bulk formation EC increases in the saturated aquifer unit, in agreement with Archie's Law (Archie 1942). This trend is evident in all the EC logs and water quality profiles obtained at this site (except background).

Additionally, replicate logs may be run at selected locations to assess repeatability and to evaluate small scale variability in sediment type. Replicate logs were run at the E4 location about 2 m apart on different days. An overlay of the two logs (Figure S6) demonstrates the HPT-GWS logging process is repeatable, and that clay lenses in the aquifer unit of the formation often are of limited lateral extent.

### Background Log (E5) with Water Quality Data

The HPT corrected pressure ( $P_c$ ) and bulk formation EC for the background log (E5) are plotted with cation, anion, and trace element data (Figure 4). At the background location the upper approximately 36 ft display elevated EC and  $P_c$  with significant variation, again indicating a generally fine-grained unit with varying amounts of silt and sand. Below approximately 36 ft both the EC and  $P_c$  logs are generally low, flat and featureless indicating coarse grained sands and gravels (aquifer unit), except the small EC spike at 74 ft and again at 87 ft indicating fine grained lenses. No EC anomaly is evident at this location. Groundwater

specific conductance measured at selected depths are plotted with the EC log and reveal that the specific conductance also is relatively low and consistent across the saturated aquifer unit. Samples for major element cations and anions and selected trace elements were collected at three depths (40, 60, and 84 ft) across the saturated aquifer unit as a second HPT-GWS log was obtained at this location. (Alternately, a simple DP groundwater sampler [ASTM 2015b] could be used to collect these samples.) The plots of sodium+potassium and chloride, as well as calcium+magnesium and sulfate vs. depth (Figure 4) display relatively flat profiles across the aquifer at the background location. This is as expected based on the groundwater specific conductance plot and EC log. Results for uranium, barium and arsenic at this location were all below regulatory action levels indicating this aquifer could be used as a drinking water supply for the local community.

### Log at Location E4 with Water Quality Data

The E4 log was run near the northeast corner of the east pond basin (Figure 2). The HPT corrected pressure ( $P_c$ ) and bulk formation EC log are plotted with cation, anion, and trace element data for this location (Figure 5). As observed at the previous locations the upper part of the formation (0 to 30 ft here) display elevated EC and  $P_c$  with significant variation, again indicating a generally fine-grained unit with varying amounts of silt and sand mixed with clay. Below 30 ft at this location both the EC and  $P_c$  logs drop quickly.

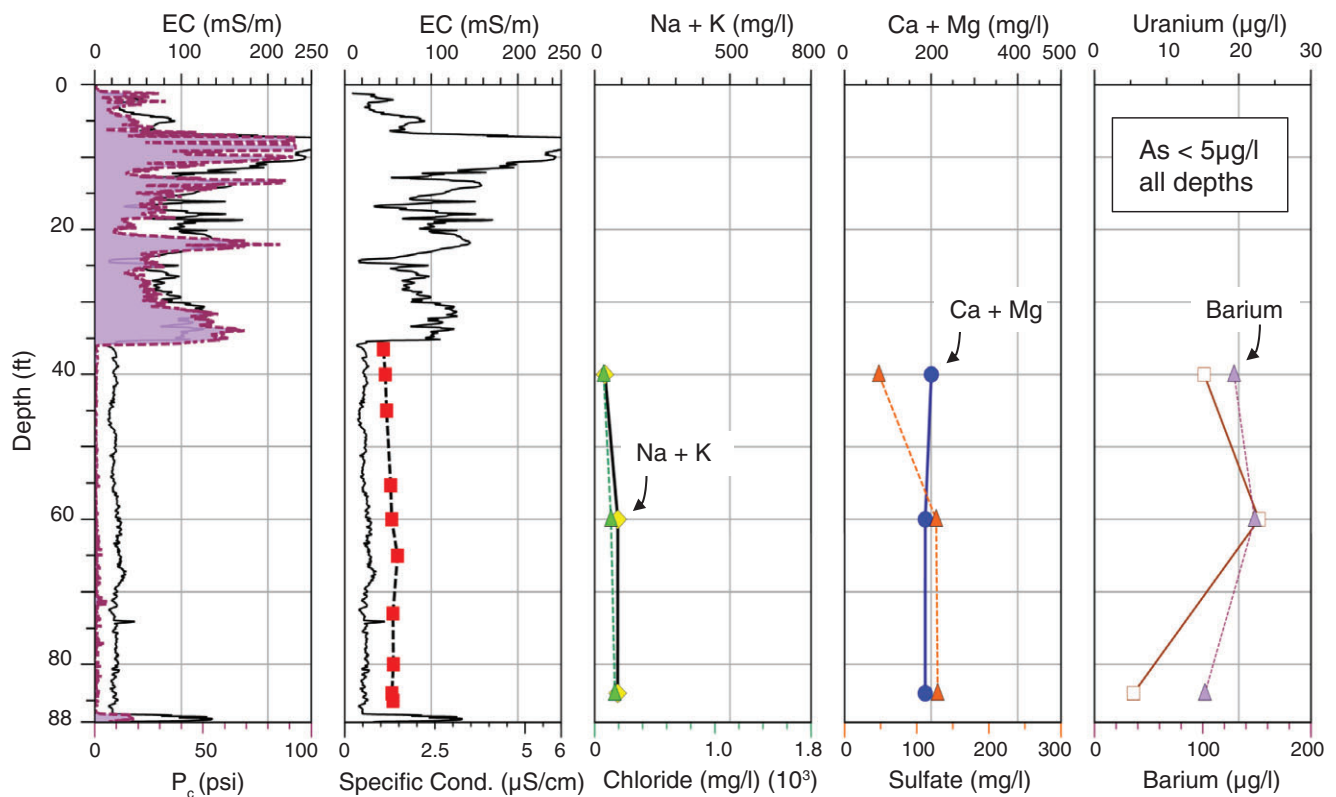


**Figure 4. EC and  $P_c$  Logs and water quality information at the background location (E5).  $P_c$  is plotted over bulk formation EC in the left panel. Below 36 ft the  $P_c$  and EC logs are generally flat and parallel, no EC anomaly. Note top and bottom scales are different for each panel. Scales are the same for Figures 4 and 5.**

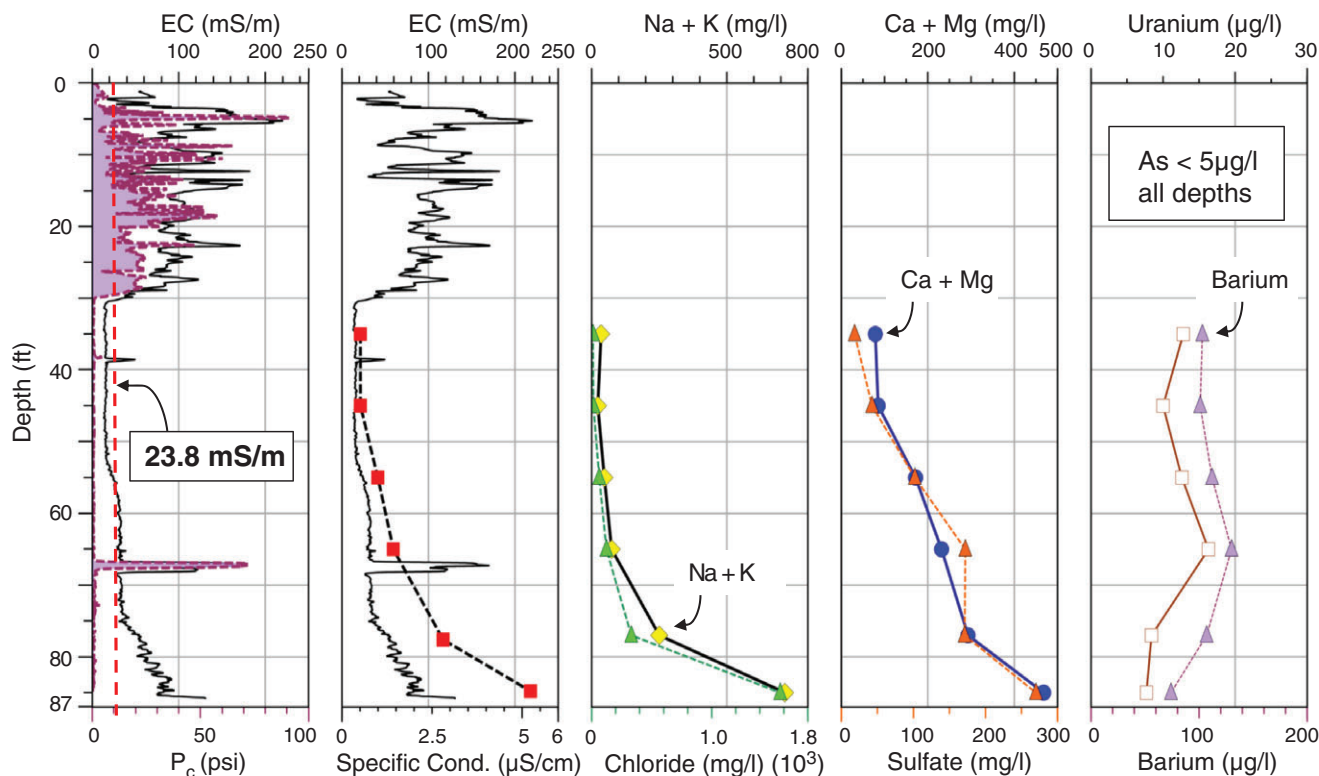


**Figure 5. Log and water quality information for location E4.  $P_c$  is plotted over bulk formation EC in the left panel. Red dashed line in the left panel is a plot of the average bulk formation EC (23.8 mS/m) for the saturated aquifer unit at the background location (E5). Between approximately 31 ft to 53 ft below grade bulk formation EC at this location (E4) is below the average background EC for the aquifer unit, indicating a negative EC anomaly over this interval. Note top and bottom scales are different for each panel. Horizontal scales are the same for Figures 4 and 5.**

Both also display peaks at about 39 ft and 67 ft indicating the presence of clay lenses. While the  $P_c$  log is otherwise low and flat the EC log displays some subtle variation vs. depth. To help distinguish the subtle variations in the EC log at this location the average bulk formation EC for the saturated aquifer unit at the background location was calculated (23.8 mS/m) and plotted as a vertical dashed line in the first panel. When the bulk formation EC in the E4 log between about 30 ft and 52 ft is compared to the background average it appears low (negative EC anomaly). Then between approximately 55 ft to 75 ft the bulk formation EC is similar to the background EC level in the saturated aquifer unit. Below 75 ft the bulk formation EC begins to increase above the background average EC while the  $P_c$  log remains low and flat, as observed at location W1 (Figure 3), again indicating a positive EC anomaly.

Stabilized groundwater specific conductance measurements (Table S1) were obtained at selected depths as the E4 log and groundwater profile were initially acquired. Plots of the specific conductance data over the EC log (Figure 5, panel 2) reveals these two parameters exhibit a similar trend, as one increases so does the other, and vice versa. Plots of the major element cations (Na+K and Ca+Mg) and anions (Cl and  $SO_4$ ) vs. depth display the same increasing trend with depth as the groundwater specific conductance in the aquifer unit of the formation. This shows that the groundwater specific conductance is controlled by the

dissolved ion concentrations as previously noted (Hem, 1985). And furthermore, the bulk formation EC in the aquifer unit is controlled by the electrical conductivity of the contained water (brine) as defined by Archie's Law (Archie 1942).

Sample results for uranium and barium at location E4 are similar, or lower than, the concentrations observed at the background location (Table S2, Figure 5) and arsenic is again nondetect at all depths. While these results indicate the water across this profile would be acceptable for use as a drinking water supply the elevated levels of sodium, chloride and sulfate observed in the sample analyses reveal that the water quality below 75 ft at this location is impaired.

#### Relationship of Dissolved Ion Concentrations to Groundwater Specific Conductance, Bulk Formation EC, and Archie's Law

Strong correlation between dissolved ion concentration and the specific conductance of surface and groundwater has been previously documented (Hem 1982, 1985). As expected, regression of groundwater specific conductance vs. dissolved ion concentrations for locations E4 and E5 at this site (Figure S7) yields a high correlation coefficient ( $R^2 > 0.99$ ). However, the presence of an extreme data pair (as seen here) can exert a strong influence on a regression analysis (Isaaks and Srivastava 1989). When the extreme data pair is removed a correlation coefficient of 0.95 is obtained for this small dataset.



Groundwater specific conductance was measured at 92 discrete intervals across 10 of the log/profile locations at this site (Figure 2 and Table S1). To assess the relationship between the bulk formation EC and groundwater specific conductance the simple math average of the bulk formation EC was calculated for one-foot (~30cm) intervals centered at each location and depth where groundwater specific conductance was measured (Table S1). A simple average for bulk formation EC was considered appropriate here since short intervals with minimal variation in the EC parameter were being modeled. Additionally, as horizontal K is typically higher than vertical K in sediments and modest volumes were purged (5 to 15L) it was considered acceptable to use only three times the actual screen interval (4-inches) for determination of the interval average bulk formation EC value for comparison to the sampled groundwater specific conductance. A plot of these paired data points (Figure 6) and regression analysis resulted in a correlation coefficient ( $R^2$ ) of approximately 0.91 with the intercept set at zero to be consistent with Archie's Law (EC of formation solids=0) (Archie 1942). Alternately, regression of the dataset without the intercept set to zero resulted in a regression line equation of  $y=0.158x+5.127$  ( $R^2=0.931$ ). The natural intercept (~5 mS/m here) may approximate the average bulk formation EC of the local aquifer unit if saturated with de-ionized water. Note that Archie's Law was originally developed to use where the connate water (brine) was over 20,000 mg/L NaCl, about 10x the maximum observed at this site. From that perspective an intercept of 5 mS/m is effectively zero.

Specifically, Archie's law (Archie 1942, 1947, 1950) was developed to relate the in situ resistivity of oil bearing, consolidated sedimentary rock (primarily sandstone) to

its porosity and brine saturation. Archie's Law assumes that the resistivity of the brine fluids controls the bulk formation resistivity and the rock/formation itself has essentially no influence on the bulk formation resistivity. In terms of electrical conductivity (the inverse of resistivity) Archie's Law may be stated as:

$$C_B = (1/\alpha) C_w \phi^m S_w^n$$

where  $C_B$  = EC of the fluid saturated bulk formation,  $C_w$  = EC of the brine (groundwater),  $S_w$  = the brine (groundwater) saturation,  $n$  = saturation exponent,  $\alpha$  = tortuosity factor (typically between 0.5 and 1.5),  $\phi$  = porosity,  $m$  = cementation exponent (typically 1.3 for unconsolidated sands) (Archie 1942, Hallenberg 1998). In this study we use  $P_c$  to help identify zones of the formation (low  $P_c$ /saturated sands-gravels) where Archie's Law would generally apply. This then allows us to use variations in EC to identify changes in water quality.

To evaluate how well the field data adhere to Archie's Law (as defined for EC above) we substituted appropriate values for porosity ( $\phi$ ) for mixed sands and gravels (between 0.20 to 0.35) (Fetter 1994) and tortuosity ( $\alpha$ ) typically ranging between 0.5 and 1.5 (Archie 1942) to obtain two models appropriate for this geologic setting. Since the formation is fully saturated with groundwater  $S_w=1.0$  for these models while the cementation factor ( $m$ ) is typically around 1.3 for unconsolidated sands (Archie 1942, Hallenberg 1998). We substituted in the measured EC of the groundwater samples ( $C_w$ ) and solved for the bulk formation EC ( $C_B$ ). The calculated models effectively bracket the regression line of the field data (Figure 6). The results clearly indicate the DP

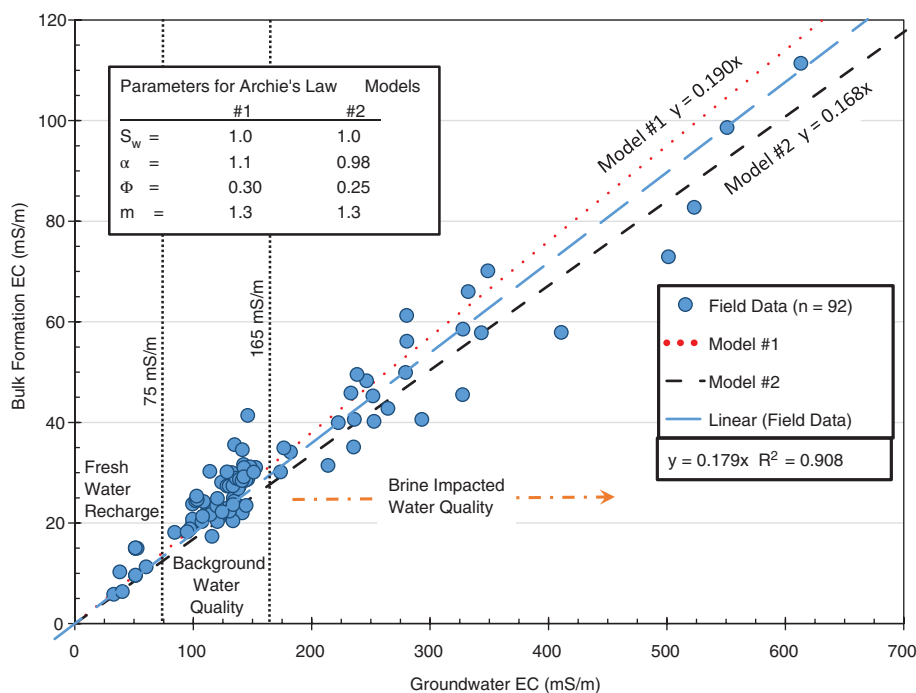


**Figure 6. Correlation of averaged bulk formation EC with stabilized groundwater specific conductance measured at multiple depths for 10 locations ( $n=92$ ) at the field site. The bulk formation EC was averaged over a one-foot interval centered at the depth where the groundwater specific conductance was measured. Geologically appropriate Archie's Law models were found to bracket the regression line of the field data.**



EC log data are consistent with Archie's Law, even at the relatively low EC of the system. Therefore, the groundwater (brine) EC is controlling the bulk formation EC in the saturated aquifer unit at this site (excluding clay layers). This relationship is probably true for similar unconsolidated sand and gravel aquifers at other sites, but further work would be required to confirm this assertion. Additionally, for sites with much higher brine concentrations the calibration for the DP EC array may need to be modified to obtain a linear fit for the site-specific conditions.

### Corrected Pressure ( $P_c$ ) Logs and Hydrostratigraphy

Due to the presence of the brine in the local aquifer and its influence on the EC logs (Figures 3, 4, 5, and 6) use of the EC logs for lithologic and hydrostratigraphic interpretation are not always effective at this site. Also, not all clays or fine grained formations will exhibit high electrical conductance and as such can be almost indistinguishable from coarse-grained materials on an EC log (McCall et al. 2014). In these situations, the  $P_c$  log provides a more reliable indicator of changes in formation permeability and sediment type. Cross sections of  $P_c$  logs may be prepared to assess both vertical and lateral changes in sediment type and hydrostratigraphy (Figure 7) when confirmed by targeted

coring or logs from previous nearby borings. Based on this cross section the base of, and changes in thickness of, the upper fine-grained unit can be traced across the site. The distribution and changes in the thickness of the aquifer unit (Table S3) also may be mapped across the site and volumes could be estimated with a 3-D plot. From the cross section it is evident that clay layers within the aquifer unit vary in thickness, usually occur below 60 ft depth (~890 ft elev.), and are generally discontinuous across the site. Also, the top of the shale bedrock can be traced in cross section and could be mapped with a 3-D plot. This capability could be useful for locating depressions in the bedrock surface where dense nonaqueous phase liquid (DNAPL) pools could form. Conversely, dome or saddle-shaped features in overlying clay rich units, as observed below the west pond basin (Figure 7), could essentially create stratigraphic traps for LNAPLs, as previously demonstrated with DP EC logs (EPA 2000).

### Mapping Groundwater Quality Based on EC and $P_c$ Logs

Having determined that the  $P_c$  logs provide good representation of sediment type at this site and that groundwater specific conductance controls the bulk formation EC for the aquifer unit at this site (and probably other similar sites) we can now use the rapidly obtained, high density log

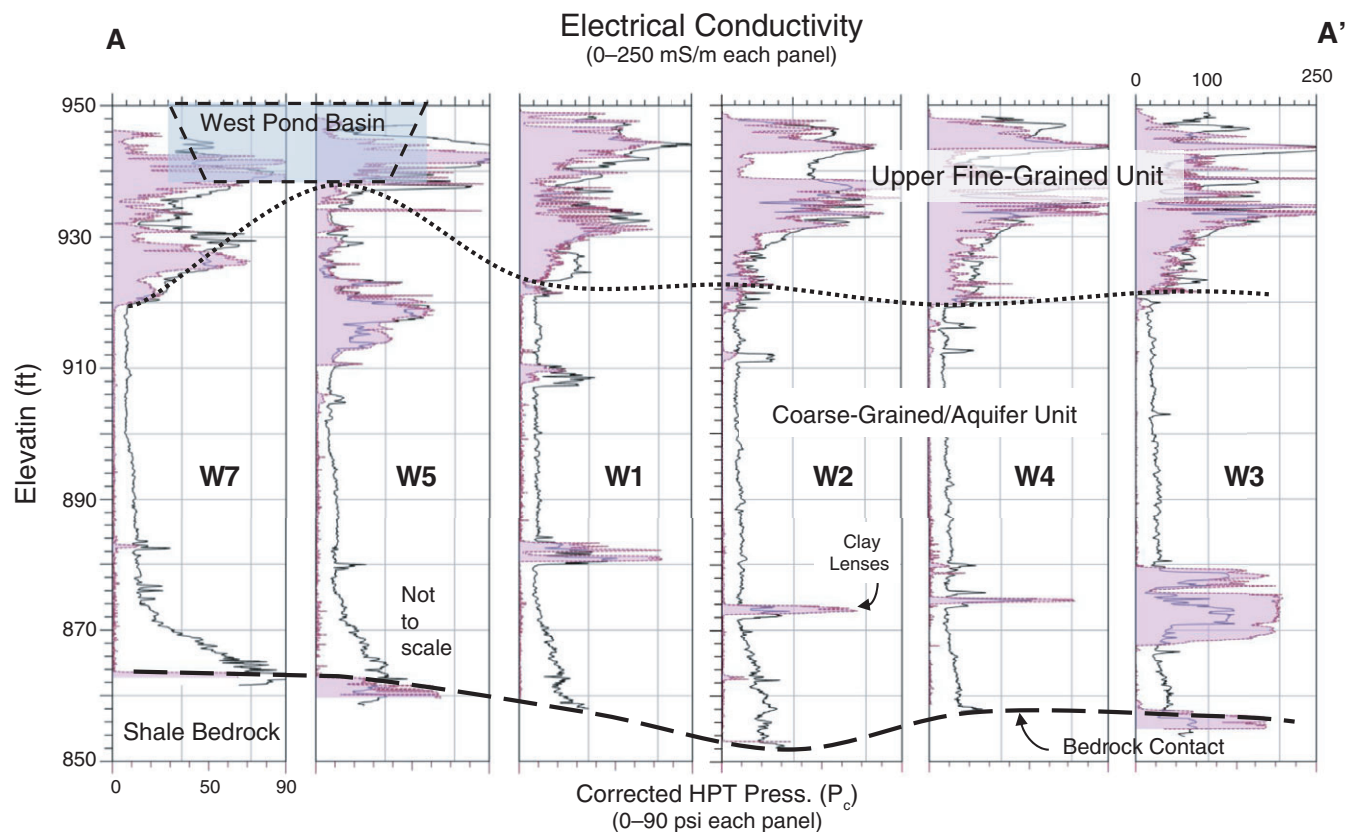


**Figure 7.** North-south cross section A-A' plotted at elevation (see Figure 2 for location). HPT corrected pressure ( $P_c$ /purple) plotted over bulk formation EC logs (white filled black line). Below approximately 75 ft EC increases while  $P_c$  remains flat until reaching the shale. In this interval EC is not a reliable indicator of lithology due to brine impact. Heavy dashed line defines contact between the aquifer unit and underlying shale bedrock. Bedrock contact with the shale was defined by use of the  $P_c$ , EC, injection flow and speed graphs at each location. Bold dotted line ( $EC=50$  mS/m) used to define contact between the upper fine-grained and coarse-grained (aquifer) unit. Blue filled box defines approximate depth and extent of west pond basin. Lateral spacing here is plotted equally, actual log spacing on the ground is not equal, not to scale.

data for EC and  $P_c$  to assess groundwater quality across the studied area in the aquifer unit. We observed at location E4 (Figure 5) that the bulk formation EC between approximately 30 to 52 ft was below the average background EC (negative EC anomaly). Additionally, the cation and anion concentrations and groundwater specific conductance were also low over this interval as compared to background results (Figure 5, Tables S1 and S2). A cross section (Figure 8) around the east and south edges of the east pond basin (B-B', see Figure 2 for location) was prepared with EC logs and groundwater specific conductance data. This cross section reveals that the low EC zone extends south around the east pond basin and then to the west (W5) beneath the west pond basin. The low EC zone is shaded pale green to define its approximate lateral and vertical extent. A red dashed line defines the base of the upper fine-grained unit on the cross section. This indicates that the fine-grained unit is thinnest at the E2 location and the bottom of the pond basin essentially penetrates this lower permeability material here. This feature enables rain water runoff (with low specific conductance) directed to the pond basin to quickly and efficiently recharge the local aquifer leading to the low EC zone observed in the formation. This is supported both by the low groundwater specific conductance measured over this zone at locations E1, E2, E3,

E4, and W5 as well as the low cation and anion concentrations observed over this zone at the E4 location (Tables S1 and S2, Figures 5 and 8).

Brine impact was observed near the base of the aquifer in several logs at the site (Figures 3, 5, 7, and S6) as defined by elevated EC and low  $P_c$ . A plot of groundwater specific conductance vs. depth for ten locations across the site demonstrated that brine impact occurred primarily below 75 ft depth (~875 ft elev.) in the aquifer unit (Figure S3). Cross section C-C' (Figure 9) traverses the north edge of the study area (see Figure 2 for location). At contact with the bedrock  $P_c$  increases, HPT flow decreases and EC generally increases. These log responses were used to define the top-of-rock (Table S3), defining the contact between the aquifer unit and the underlying shale bedrock. For several feet above bedrock contact at most locations the EC is elevated while  $P_c$  remains low and flat, defining brine impact at the base of the aquifer. The brine impact zone is shaded pink on the cross section. It is interesting to note that the brine impact zone tends to follow the bedrock topography, suggesting that the shale may be the brine source. The area of low EC resulting from freshwater recharge is shaded light green on this cross section, providing approximate east-west extent for the recharge lens. At location W6 the

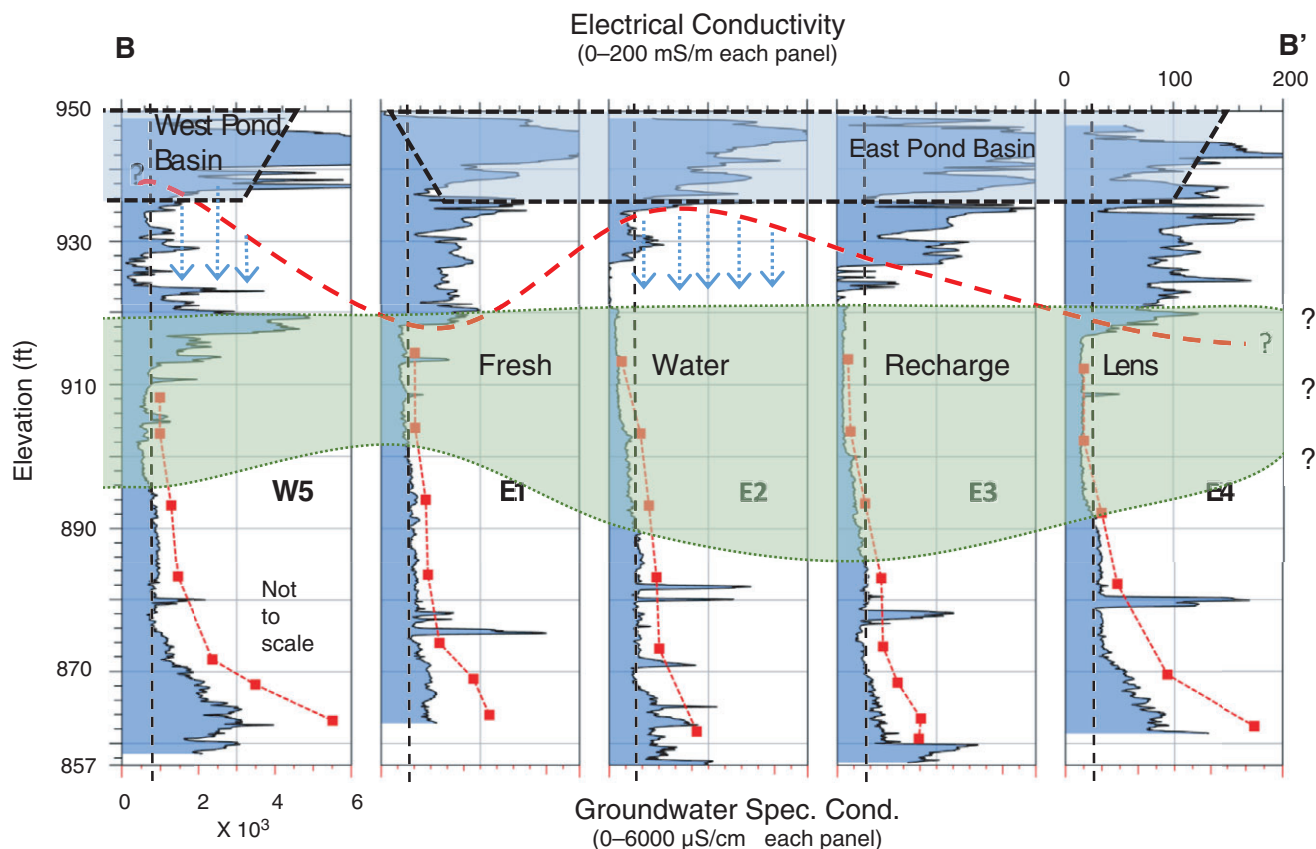


**Figure 8.** Cross section B-B' with EC logs shaded in blue, plotted at elevation (see Figure 2 for location). Red lines with red boxes = groundwater specific conductance. Vertical black dashed line on each log represents the average EC for the saturated aquifer facies at the background location (23.8 mS/m). Bold red dashed curve = base of clay rich, fine-grained facies, based on EC = 50 mS/m. Light blue shaded blocks depict the approximate extent & depth of the pond basins. Dotted arrows indicate where base of pond lies close to bottom of fine-grained facies, permitting efficient recharge to the local aquifer. Light green shaded area defines the zone where fresh water recharge from the pond basins have lowered the bulk formation EC below the background average EC. Log spacing in cross section plotted as equal, actual spacing on the ground is not equal. Not to scale.

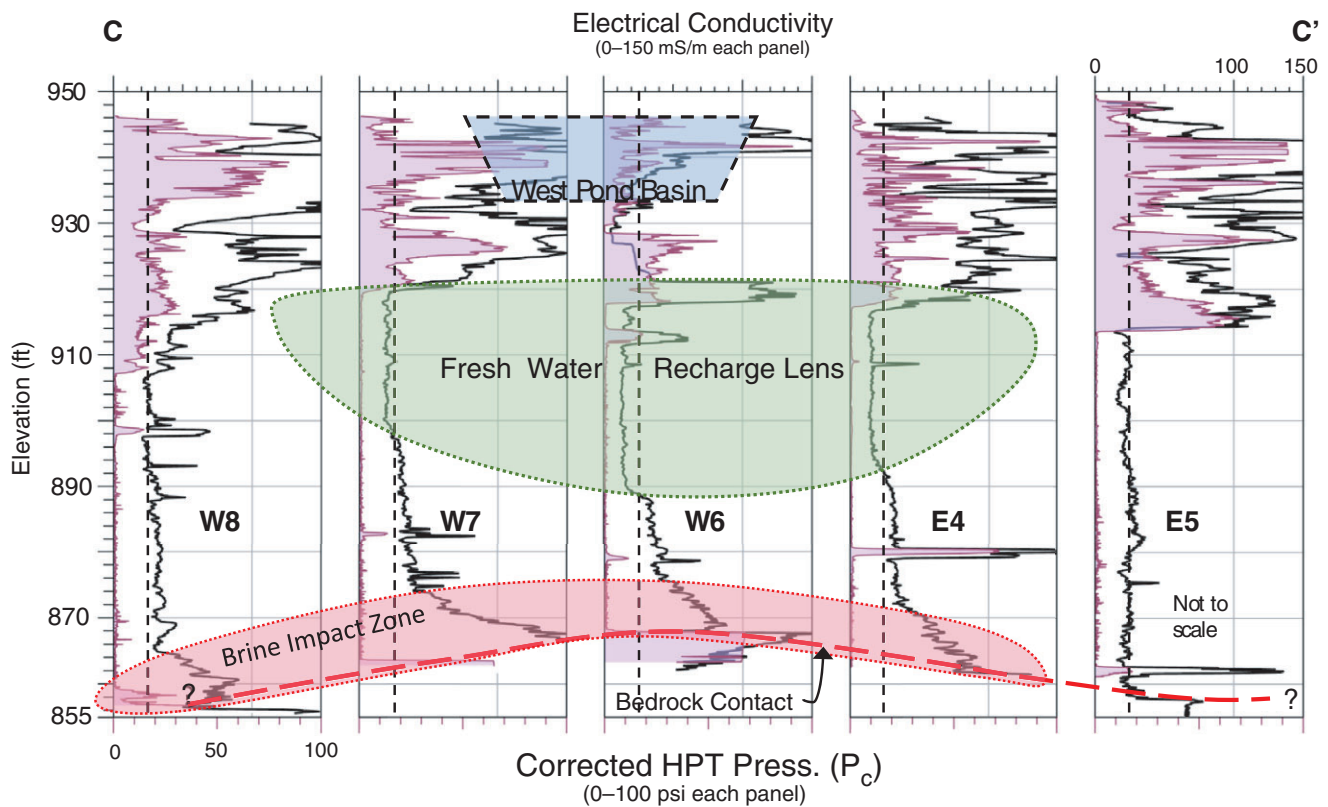


**Figure 9.** West to east cross section C-C' along north boundary of investigation area plotted at elevation (See Figure 2 for Location). EC logs=black line with white fill,  $P_c$ =purple. Vertical black dashed line on each log represents the average EC for the saturated aquifer facies at the background location (23.8 mS/m). Blue shaded block depicts the approximate extent & depth of the west pond basin. Light green shaded area generally defines the fresh water recharge lens,  $EC < 23.8$  mS/m except for clay layers and where groundwater level intersects base of fine grained facies. Pink shaded area outlines zone at base of aquifer facies impacted by brine ( $EC > 50$  mS/m,  $P_c < 5$  psi). Log spacing in cross section plotted as equal, actual spacing on the ground is not equal. Not to scale.

bottom of the west pond basin appears to penetrate through the thin upper fine-grained unit into silty-sandy material (low EC and  $P_c$ ) providing a possible avenue for rapid recharge beneath this pond basin. Also note the abrupt change in bulk formation EC at location W6 between approximately 888 ft and 890 ft elevation with no change in  $P_c$ . This indicates a sharp transition between the fresh water recharge and brine impact at this depth/location.

To better characterize the areal extent of the groundwater recharge lens and the brine impact shading was applied to the site map (Figure S8). The N-S extent of the brine plume in the study area is largely defined by contrasting the EC and  $P_c$  logs (Figures 3, 5, 7, and 9) which indicates the southern edge of brine impact is just south of Log W3. The E-W trend of the brine plume is largely defined by contrasting the EC and  $P_c$  logs in cross section (Figure 9) in the study area. The extent of brine impact is shaded pink on the map (Figure S8) and it appears to continue north of the studied area but terminates between logs E4 and E5 on the east and appears to be pinching out just west of location W8 and south of location W3.

Additionally, the extent of the freshwater recharge plume is defined by the low bulk formation EC and groundwater specific conductance (Figures 5, 8, and 9, Table S1) as contrasted to the background levels for this formation (Figure 4). The recharge lens (Figure S8) may extend further to the north

but additional logs would need to be obtained to confirm this hypothesis. Furthermore, the effects of fresh water recharge appear to extend deeper into the aquifer unit around logs E2, E3, E4, and W6 (Figures 8 and 9) as the bulk formation EC and groundwater specific conductance data are low in these zones as compared to other logs (W1 to W4, W8, E1, and E5) at the site. The plot of bulk formation EC vs. groundwater specific conductance (Figure 6) and groundwater specific conductance vs. depth (Figure S3) also help to define water quality zones (fresh water recharge, background, brine impact) in the aquifer unit.

## Summary and Conclusions

The HPT-GWS system enables a site investigator to obtain electrical conductivity (EC) logs simultaneously with HPT injection pressure logs as the probe is advanced into unconsolidated formations with DP methods. The 20 screened injection/sample ports on the probe enable the investigator to stop at multiple depths as the log is being run and use the down-hole pump to purge and monitor water quality and collect groundwater samples. Formation permeability must be sufficient to yield water for sampling and the EC and pressure logs are used to identify zones of interest as logging is performed. Samples for many analytes or low level contaminants of interest can be collected, as demon-



strated by the major element cation, anion and low concentration arsenic, barium, and uranium results at this site.

In fact, the limited analytical data at this site indicates that the surface water recharge is not mobilizing either arsenic or uranium from the upper fine grained unit during infiltration. This suggests the groundwater from the recharge zone would be acceptable as a drinking water supply. Additional sampling across the recharge area would be useful to confirm the limited data. Also, the few samples from the brine impacted zone do not show elevated arsenic or uranium. However, elevated levels of sodium, chloride, and sulfate in the brine impacted zone (below 75 ft depth) would not make this an attractive source of drinking water. Assuming no significant increases of brine infiltration and continued fresh water recharge, shallow wells screened several feet above the brine impact could provide modest supplies of good water for residential, farm, or small businesses in this area.

In many unconsolidated formations where fresh water prevails HPT corrected pressure logs ( $P_c$ ) and electrical conductivity logs closely correspond and independently confirm one another. Typically, high EC and  $P_c$  results indicate increased clay content and lower permeability in these settings. Conversely, low EC and  $P_c$  usually indicate coarse grained materials with higher permeability. Under these formation conditions a few targeted core samples (ASTM 2015a) may be used to confirm the logs and the logs may then be used to interpret the distribution of sediment types across the larger investigation area. The next step is the construction of cross sections, fence diagrams and/or 3D models based on the logs to obtain a high-resolution site model of the local hydrostratigraphy. These models can be used to guide the selection of screen intervals for water supply wells, or locate monitoring wells or temporary DP piezometers (ASTM 2015b) for purposes of environmental investigation. These hydrostratigraphic models also can be used to define migration pathways or hydraulic barriers (e.g., aquitards) and help develop a remediation strategy for many contaminated sites.

However, there are some clay minerals that do not exhibit high electrical conductance and elevated dissolved ion concentrations (brine, seawater intrusion, sodium persulfate injections, etc.) can cause elevated EC readings in saturated sands and gravels. Even under conditions causing EC anomalies or where low EC clays predominate, the  $P_c$  log will still provide representative information about formation permeability. From a useful perspective contrasting  $P_c$  logs to EC logs can be conducted to identify EC anomalies. As reviewed here contrasting the  $P_c$  and EC logs can help identify not only positive EC anomalies but also negative EC anomalies with lower than normal bulk formation EC in saturated coarse-grained formations. The relatively low EC readings (as compared to background conditions) together with water quality data obtained while logging identified fresh water recharge to the local unconsolidated aquifer from two storm water retention basins. Then cross sections based on several logs across the area spatially defined the vertical and areal extent of the freshwater recharge lens based on the EC and  $P_c$  log results. Additionally, siting of aquifer recharge basins or recharge wells for unconsolidated aquifers could be accomplished effectively with an HPT-GWS investigation program.

At the studied site relatively small positive EC anomalies (EC elevated/ $P_c$  low) observed in individual logs were used to identify brine impact at the base of the alluvial aquifer. Again, water quality data obtained at targeted locations and depths as the logs were conducted confirmed increases in groundwater specific conductance and major element cation/anion concentrations to verify the brine impact. A simple regression of groundwater specific conductance data against bulk formation EC measured at the same intervals in the saturated coarse-grained “aquifer” unit of the formation yielded a correlation coefficient ( $R^2$ )=0.93 for the area investigated. Two models based on Archie’s Law (Archie 1942) with geologically appropriate parameters were found to bracket the regression line of the field data. This confirmed that the groundwater specific conductance exerts a controlling influence on the bulk formation EC of the aquifer unit at this site. This relationship is probably true for many sites with similar formation (siliceous sands and gravels) and groundwater conditions. By contrasting the EC and  $P_c$  logs at each location the vertical extent of the brine impact could be identified. Then cross sections of the logs were used to track the distribution of the brine plume in the subsurface and finally to map the areal distribution of the brine. In the limited area studied the brine impact appeared to mimic the topography of the shale bedrock, suggesting the shale may be the source of the brine. Additional investigation would be required to confirm this hypothesis. The combination of the EC and HPT pressure log data along with the water quality data and sample results from the HPT-GWS probe provide a useful tool for those involved with subsurface investigation of unconsolidated formations and aquifers. Application of the field methods and data analysis methods described here should prove useful for many hydrogeologic and groundwater quality/contaminant investigations. Additionally, further research with the DP EC logs and  $P_c$  logs along with the application of Archie’s Law may prove useful for helping to determine the presence of nonaqueous phase liquids (NAPL) in some unconsolidated formations.

## Acknowledgments

The authors would like to express their appreciation to the editorial and technical reviewers (especially Seth Pitkin and Everton de Oliveira) for their valuable input and suggestions which lead to improvements in the manuscript. We would also like to express our appreciation to Martha Tasker, Director of Utilities, and Dan Stack, City Engineer for their support and for providing access to the City of Salina, Kansas property where this work was conducted. The first two authors work for the manufacturer of the HPT-GWS probe.

## Supporting Information

The following supporting information is available for this article:

**Figure S1.** Pressure Dissipation Test Time File

**Figure S2.** Typical Groundwater Parameter Stabilization Profile

**Figure S3.** Groundwater Specific Conductance vs. Depth

**Figure S4.** Concentration vs. Depth for Selected Major Element Cations and Anions

**Figure S5.** Uranium and Barium Concentration vs. Depth

**Figure S6.** Overlay of Replicate E4 Logs

**Figure S7.** Ion Concentration vs. Groundwater Specific Conductance

**Figure S8.** Map View of Brine Impact and Fresh Water Recharge Lens

**Table S1.** Stabilized Water Quality Data and Interval Average Bulk Formation EC

**Table S2.** Analytical Results for Groundwater Samples

**Table S3.** Formation Depths, Contact Elevations & Aquifer Thickness

## References

- American Society of Testing and Materials (ASTM) International. 2016. (WK48024: in review) Standard Practice for Direct Push Hydraulic Logging for Profiling Variations of Permeability in Soils. West Conshohocken, Pennsylvania: ASTM International. [www.astm.org](http://www.astm.org)
- ASTM. 2015a. D6282, Standard Guide for Direct Push Soil Sampling for Environmental Site Characterizations. In Volume 04.09 Soil and Rock (II). West Conshohocken, Pennsylvania: ASTM International. [www.astm.org](http://www.astm.org)
- ASTM. 2015b. D6001, Standard Guide for Direct-Push Groundwater Sampling for Environmental Site Characterization. In Volume 04.09 Soil and Rock (II). West Conshohocken, Pennsylvania: ASTM International. [www.astm.org](http://www.astm.org)
- Archie, G.E. 1950. Introduction to petrophysics of reservoir rocks. *American Association of Petroleum Geologists Bulletin* 34, no. 5: 943–961. DOI:10.1306/3d933f62-16b1-11d7-8645000102c1865d.
- Archie, G.E. 1947. Electrical resistivity an aid in core-analysis interpretation. *American Association of Petroleum Geologists Bulletin* 31, no. 2: 350–366.
- Archie, G.E. 1942. The electrical resistivity log as an aid in determining some reservoir characteristics. *Petroleum Transactions of AIME* 146: 54–62. DOI:10.2118/942054-g.
- Butler, J.J., P. Dietrich, V. Wittig, and T. Christy. 2007. Characterizing hydraulic conductivity with the direct-push permeameter. *Ground Water* 45, no. 4: 409–419.
- Chapuis, R.P., and D. Chenaf. 2003. Variable-head field permeability tests in driven casings: Physical and numerical modeling. *Geotechnical Testing Journal* 26: 245–256.
- Christy, C. D., T. M. Christy, and V. Wittig. 1994. A Percussion Probing Tool for the Direct Sensing of Soil Conductivity. Technical Paper No. 94–100. March. 16 pages. [www.geoprobe.com](http://www.geoprobe.com)
- Geoprobe. 2013. Geoprobe® Hydraulic Profiling Tool (HPT) System, Standard Operating Procedure. Technical Bulletin No. MK3137. Kejr, Inc., Salina, KS. February. 20 pages. [www.geoprobe.com](http://www.geoprobe.com)
- Geoprobe. 2011a. Application of the Geoprobe® HPT Logging System for Geo-Environmental Investigations. Technical Bulletin No. MK3184. [www.geoprobe.com](http://www.geoprobe.com)
- Geoprobe. 2011b. Geoprobe® Model MB470 Mechanical Bladder Pump, Standard Operating Procedure. Technical Bulletin No. MK3013. Salina, Kansas: Kejr Inc. [www.geoprobe.com](http://www.geoprobe.com)
- Dietrich, P., J.J. Butler Jr., and K. FaiB. 2008. A rapid method for hydraulic profiling in unconsolidated formations. *Ground Water* 46, no. 2.
- Dietze, M., and P. Dietrich. 2012. Evaluation of vertical variations in hydraulic conductivity in unconsolidated sediments. *Ground Water* 50, no. 3: 450–456.
- Dobrin, M.B. 1976. *Introduction to Geophysical Prospecting*. New York: McGraw-Hill.
- Fetter, C.W. 1994. *Applied Hydrogeology*, 3rd ed. Upper Saddle River, New Jersey: Prentice-Hall, Inc.
- Hallenberg, J.K. 1998. *Standard Methods of Geophysical Formation Evaluation*. Boca Raton, Florida: Lewis Publishers.
- Hem, J. D. 1985. Study and Interpretation of the Chemical Characteristics of Natural Water, 3rd ed. USGS Water Supply Paper 2254. Washington, DC: U.S. Government Printing Office.
- Hem, J.D. 1982. Conductance: A collective measure of dissolved ions. In *Water Analysis*. Inorganic Species pt. 1, Vol. 1, ed. R.A. Minear and L.H. Keith, 137–161. New York: Academic Press.
- Isaaks, E.H., and R.M. Srivastava. 1989. *An Introduction to Applied Geostatistics*. New York: Oxford University Press.
- Kansas Geological Survey (KGS). 2000. Generalized Geologic Map of Kansas. Lawrence, Kansas: The University of Kansas. [www.kgs.ukans.edu](http://www.kgs.ukans.edu)
- Kansas Geological Survey (KGS). 1952. Geology and Groundwater Resources of Lincoln County, Kansas. Bulletin 95. Univ. of Kansas Publications, State Geological Survey of Kansas.
- Kansas Geological Survey (KGS). 1949. Ground-Water Conditions in the Smoky Hill Valley in Saline, Dickinson, and Geary Counties, Kansas. Bulletin 84. Univ. of Kansas Publications, State Geological Survey of Kansas.
- Keys, W.S. 1997. *A Practical Guide to Borehole Geophysics in Environmental Investigations*. Boca Raton, Florida: CRC Press/Lewis Publishers.
- Kober, R., G. Hornbruch, C. Leven, L. Tischer, J. Grobmann, P. Dietrich, H. Weib, and A. Dahmke. 2009. Evaluation of combined direct-push methods used for aquifer model generation. *Ground Water* 47, no. 4: 536–546.
- Liu, G., J.J. Butler Jr., E. Reboulet, and S. Knobbe. 2011. Hydraulic conductivity profiling with direct push methods. *Grundwasser – Zeitschrift der Fachsektion Hydrogeologie*. DOI:10.1007/s00767-011-0182-9.
- McCall, W. 2005. Evaluation of a small mechanical and pneumatic bladder pump for water quality sampling. *Groundwater Monitoring & Remediation* 25, no. 2: 142–153.
- McCall, W., T.M. Christy, D. Pipp, M. Terkelsen, A. Christensen, K. Weber, and P. Engelsen. 2014. Field application of the combined membrane-interface probe and hydraulic profiling tool (MiHpt). *Groundwater Monitoring & Remediation* 34, no. 2: 85–95.
- McCall, W., T.M. Christy, T. Christopherson, and H. Issacs. 2009. Application of direct push methods to investigate uranium distribution in an alluvial aquifer. *Groundwater Monitoring & Remediation* 29, no. 4: 65–76.
- Milsom, J., and A. Eriksen. 2015. *Field Geophysics*, 4th ed. Hoboken, New Jersey: Wiley Blackwell.
- Pitkin, S.E., J.A. Cherry, R.A. Ingleton, and M. Broholm. 1999. Field demonstrations using the waterloo ground water profiler. *Groundwater Monitoring & Remediation* 19, no. 2: 122–131.
- Reiffsteck, P., B. Dorbani, E. Haza-Rozier, and J.-J. Fry. 2010. A new hydraulic profiling tool including CPT measurements. In *Presented at the 2<sup>nd</sup> International Symposium on Cone Penetration Testing*. Volume 2: Equipment and Procedures, Paper No. 1–11, 8 pages. [www.cpt10.com/cpt10pdfpapers.html](http://www.cpt10.com/cpt10pdfpapers.html)
- Rhoades, J.D., and J. Schilfgaarde. 1976. An electrical conductivity probe for determining soil salinity. *Soil Science Society of America* 40: 647–651.
- Sherman, H.M., J.S. Gierke, and C.P. Anderson. 2007. Controls on spatial variability of uranium in sandstone aquifers. *Groundwater Monitoring & Remediation* 27, no. 2: 106–118.

- Smith, A.H., E.O. Lingas, and M. Rahman. 2000. Contamination of drinking water by Arsenic in Bangladesh: A public health emergency. *Bulletin of World Health Organization* 78: 1093–1103.
- U.S. Environmental Protection Agency (EPA). 2016. Table of Regulated Drinking Water Contaminants. <https://www.epa.gov/your-drinking-water/table-regulated-drinking-water-contaminants#Inorganic> (accessed March 30, 2016).
- U.S. Environmental Protection Agency (EPA). 2001a. Radionuclides Rule: A Quick Reference Guide. Office of Water. EPA 816—F-01-013
- U.S. Environmental Protection Agency (EPA). 2001b. EPA Technical Fact Sheet: Final Rule for Arsenic in Drinking Water. Office of Water (4607). EPA 815-F-00-016.
- U.S. Environmental Protection Agency (EPA). 2000. Innovations in Site Characterization: Geophysical Investigation at Hazardous Waste Sites. OSWER 5102G. EPA-542-R-00-003. August. [www.epa.gov/tio](http://www.epa.gov/tio), [clu.in.org](http://clu.in.org)
- Welch, A.H., D.B. Westjohn, D.R. Helsel, and R.B. Wanty. 2000. Arsenic in groundwater of the United States: Occurrence and geochemistry. *Ground Water* 38: 589–604.

## Biographical Sketches

**Wesley McCall**, corresponding author, is at Geoprobe Systems, Inc., 1835 Wall St., Salina, KS 67401; 785-404-1147; [mccallw@geoprobe.com](mailto:mccallw@geoprobe.com)

**Thomas M. Christy** is at Geoprobe Systems, Inc., 1835 Wall St., Salina, KS 67401; 785-404-1146; [christyt@geoprobe.com](mailto:christyt@geoprobe.com)

**Mateus Knabach Ewald** is at Universidade Federal de Pelotas, Rua Andrade Neves 1948, Pelotas, 96020040, RS, Brazil; +555399768787; [mateusknabach@gmail.com](mailto:mateusknabach@gmail.com)